Journal of Mines, Metals and Fuels, *71(12C) : 302-306; 2023. DOI: 10.18311/jmmf/2023/47251*

Print ISSN : 0022-2755

Journal of Mines, Metals and Fuels

Contents available at: *www.informaticsjournals.com/index.php/jmmf*

Size Control of Silver Nanoparticles Synthesized by UV Irradiation Technique from Silk Fibroin

C. S. Shivananda[1], G. Poojitha[2] and S. Madhu[2]

[1]Research and Development Center, Department of Physics, Sir M. Visvesvaraya Institute of Technology (Affiliated to Visvesvaraya Technological University, Belagavi), Bengaluru - 562 157, Karnataka, India; shivananda_phy@sirmvit.edu, shivu.msc@gmail.com

[2]Department of Physics, Manipal Institute of Technology, Manipal Academy of Higher Education, Manipal - 576104, Karnataka, India

Abstract

This paper presents a standard protocol for the fabrication of biocompatible metal silver nanoparticles (AgNPs) by utilizing protein biomaterials Silk Fibroin (SF) under Ultra-Violet (UV) environment. The silk protein solution has good reducing and stabilizer for the formation of AgNPs. The duration of UV exposure influences the size and shape of the AgNPs. The plasmonic resonance band observed around 425-430 nm is validated from UV-Vis absorption studies and it confirms the conversion of Ag^{+} to Ag° in silk fibroin solution. AgNPs are evenly dispersed in the SF solution with narrow sizes, as evident by Transmission Electron Micrographs (TEM). The UV exposure time significantly impacted on the size reduction of Ag nanoparticles for medical and electronic device applications.

Keywords: Silver Nanoparticle, Silk Fibroin, TEM, UV-Visible

1.0 Introduction

The potential applications in area of nanotechnology silver nanoparticles have recently received much more interest in the area of electronics and biomedicine. The main advantages of these nanoparticles are their carrier transport properties, optical, mechanical, thermal, and magnetic properties[1-5]. Noble metallic silver nanoparticles are associated with one another in terms of size, shape, structure, and particle distribution. Additionally, they exhibit a high surface-to-volume ratio and outstanding Surface Plasmon Resonance (SPR) properties[6,7]. Metallic nanoparticles can be synthesized by a variety of techniques, including photon-induced reduction, reducing agents in a liquid suspension with different polymer solvents, chemical reduction in solid materials like mesoporous silicate or in natural fibres like micelles, chemical vapour deposition, UV, microwave, x-ray, and ultrasound radiation, and the synthesis of polymer-based nanocomposites. Since they provide stability against oxidation, agglomeration, and precipitation, many polymers are useful as stabilizers[8]. The method of fabrication of metal nanoparticles *via* UV irradiation reduction has a number of benefits. Through the utilization of hydrated electrons formed during irradiation in the solution, metal ions can be converted into metal particles with no vacancies[9]. Some studies have suggested that metallic nanoparticles can alter their size and shape as well as form extremely tiny micro aggregates when radiation-assisted nucleation growth[10-13]. The UV irradiation technique is influenced by a number of variables, including wavelength, energy, and irradiation methods[14-18]. The impact of UV irradiation period can aid to control the size of AgNPs. In the present study, SF was utilized to synthesize AgNPs while being exposed to UV light as a reducing agent and a green stabilizer. The duration of UV

**Author for correspondence*

exposure has an impact on AgNPs size, physio-chemical, and biological activities. This has a significant impact on AgNPs size and shape. The synthesized nanoparticles were subjected to UV-V is, TEM, and EDS methods in order to assess the plasmonic properties, surface morphology, size and diffraction pattern, and elemental signal peaks of the AgNPs in the SF matrix, respectively[19].

2.0 Experimental Methods

2.1 Materials

Na_2CO_3, LiBr and $AgNO_3$ (99%) were purchased from Merck and utilized without further purification. The FC_2 cross breed silk - (*Bombyx mori*), multivoltine cocoons were purchased from Government Cocoon Market, Ramanagra, Karnataka, India.

2.2 Degumming of Synthesis of Silk Fibroin (SF)

The sericin-gumming protein content was removed by cutting the *Bombyx mori* silk cocoons into tiny pieces and boiling them in aqueous sodium carbonate (Na_2CO_3) solutions for 60 minutes at a time. In order to get pure SF, the degummed bundle of sericin-free SF fibre is washed in double-distilled water to remove impurities. It is then allowed to dry at room temperature for 24 hours. To prepare SF solution, 2 gram of dried fibre was dissolved in desired concentration of an aqueous LiBr solution, which was then heated to 60 °C for 4 hours. As a result of the treatment, Li ions enter the silk fibroin crystal domain and contaminate the solution obtained by this treatment[20]. To produce an ion-free solution, the SF solution requires being dialyzed using de-ionized water for 72 hours at room temperature. During the treatment, the optically clear solution was centrifuged for approximately 20 minutes at 4000 r/min in order to extract the undissolved silk content that collects at the bottom of the centrifuge tube. The pure SF solution was then placed at 4°C so it could be used for further process. By adding deionized water, the SF solution's concentration which was around 20 wt % was lowered to 5 wt %.

2.3 Preparation of Silk Fibroin - Ag Nanoparticles (SF-AgNPs) Solution

A 5 wt% silk fibroin solution was mixed with a predetermined concentration of silver nitrate ($AgNO_3$) salts (5 mg/mL), resulting in a clear Silk Fibroin-silver nitrate solution (SF-$AgNO_3$). The resultant solution mixture was subjected to UV light with a 315-280 nm wavelength range. To synthesize a colloidal solution of SF-AgNPs, different radiation exposure times were performed for the suspension containing silk fibroin and silver nitrate (SF-$AgNO_3$). Ag Nanoparticles size, shape, and production may vary depending on how long the UV light is exposed the final composite solution was observed to be stable at room temperature.

3.0 Characterization Techniques

3.1 UV-Visible analysis

Silk fibroin-Ag nanoparticle (SF-AgNPs) samples were investigated by measuring the samples' absorption spectra in the 190-800 nm wavelength range using a UV-Vis spectrophotometer (Shimadzu UV-1800, Japan).

3.2 Transmission Electron Microscopy

With a JEOL - TEM 2100 LaB_6 and an accelerating voltage of 200 keV, was employed to investigate at the nanoparticles size and morphology. Colloidal SF-AgNPs solution is sprayed over carbon-coated copper grids for TEM analysis, and the grids are then allowed to dry under an infrared light.

4.0 Results and Discussion

In the current study, silver nanoparticles were formed by UV light exposure, and silk fibroin was employed as an effective co-reductant and stabilizer in the AgNPs formation[20]. Here, we investigated how UV radiation exposure impacted AgNPs size-dependent characteristics. In the SF-$AgNO_3$ solution, the metallic salts first dissociated, then it is subjected to UV light exposure, these metallic salts break down into smaller particles that are stabilized by the amino acid residues in silk fibroin, giving rise to AgNPs[19]. Aqueous silk fibroin solution that contains $AgNO_3$ as a reducing agent forms solvated electrons when exposed to UV light. It finally achieves a stable state when these electrons combine to form agglomerates that reduce the silver cations to silver atoms. The reaction mechanism is shown here[21-23].

$$AgNO_3 \rightarrow Ag^+ + NO_3^- \text{ (Dissociation)} \quad (1)$$

$$n.H_2O \rightarrow e_{aq}^- + H^+ + OH^- + H_3O^+ + H_2 + \cdots,$$

(Irradiation) (2)

$$Ag^+ + e^-_{aq} \rightarrow Ag^0 \text{ (Reduction)} \quad (3)$$

The process by which the neutral silver atoms (Ag°) reduce from silver ions (Ag^+) and forms clusters of Ag as shown below[18].

$$Ag^0 + Ag^+ \rightarrow Ag_2^+ \quad (4)$$

$$nAg^+ + Ag_2^+ \rightarrow (Ag)_n^+ \quad (5)$$

$$(Ag)_n^+ + ne^-_{aq} \rightarrow (Ag)_n \quad (6)$$

The transparent Ag^+/SF solution changes to pale yellow in the exposed to UV light suggests that stable AgNPs are being produced in the composite SF solution[24].

4.1 UV-Visible Study

Among 18 amino acid residues that comprise silk fibroin, Tyrosine (Tyr) is a potent electron-donor and is involved in the conversion of Ag^+ to Ag° neutral atom[25]. This work used UV light as a technique to accelerate AgNPs formation and size reduction. The absorption spectra of a pure SF and colloidal solution of SF-AgNPs are as shown in Figure 1. Pure SF (not shown in the image) has an absorption peak at 275 nm, which is mostly ascribed to amino acid residues in the chain undergoing an electron transition[26]. Figure 1 show a typical Surface Plasmon Resonance (SPR) absorption band can be seen, this results from the formation of AgNPs with a spherical shape. The location of the most significant absorption band resulting from the activation of surface plasmon resonance of AgNPs is used to measure the average size of the nanoparticles[27]. The particle size is determined by the width of the absorption band is determined by the area under the SPR band in Figure 1. The UV exposure time and nanoparticle concentration are increased, the absorption peak increases (Figure 1), because more silver nanoparticles have the capacity to aggregate over the silk molecule covering and form bigger particles, as increasing the exposure time the size of the nanoparticles increases. The TEM study supports this result (Figure 4).

The composite solution of SF and $AgNO_3$ transforms from colourless to pale yellow when exposed to UV light, indicating that stable AgNPs have obtained in the SF solution. Due to the formation of additional nanoparticles and a rise in the concentration of AgNPs in the silk fibroin solution, evidenced by the changes of colour from transparent pale yellow, then to brown, as the UV irradiation period was increased.

Figure 1, shows that when the UV irradiation period increased, more AgNPs were formed by increasing in the intensity of the absorption band. The average particle size appears to increase with radiation duration in Figure 3, which is induced by the accumulation of silk molecules over the AgNPs surface, resulting in the formation of fluffy particles. This increase in the size of AgNPs may also be a sign that nucleation has taken place at varied irradiation times throughout the growth phase. The decreasing in the average size of many fluffy particles and the rise in the density of tiny particles during the reduction reaction process causes the average size of the nanoparticle to decrease after a 5-hour irradiation[28].

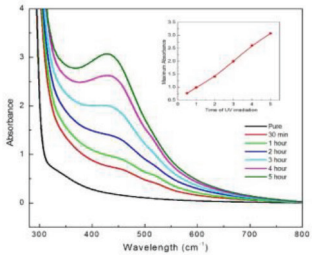


Figure 1. The spectra of SF and AgNPs.

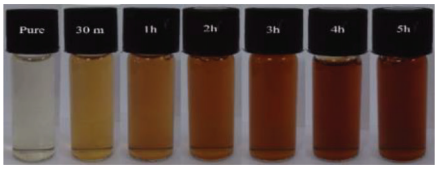


Figure 2. AgNPs in SF Solution.

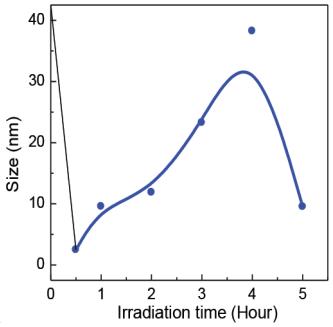


Figure 3. Variation of size of the particle with UV light exposure.

4.2 TEM Analysis

As the exposure time increases, the formed AgNPs particle size increases up to four hours; however, the particle size varies, as seen in the TEM micrograph of AgNPs. The fluffy particle size decreases after a 5-hour irradiation, which lowers the average particle size. The average size of the silver nanoparticles increases in Figure 4(a-f), with the corresponding values being 9.58, 11.87, 23.28, 40.56, and 9.56 nm. Figure 5(a-b) shows the spherical shape and smooth surface of the synthesized silver nanoparticles. The sample from Figure 5c SAED pattern demonstrated the extremely crystalline quality of formed silver nanoparticles by revealing well-defined Debye-Scherrer rings, also proving that the formed silver nanoparticles are single crystals[29]. Additionally, Figure 5d showed that the particles lattice d-spacing in the (111) plane is found to be 0.285 nm. Further, the proof of AgNPs are forming in the silk fibroin solution has been supported by the energy dispersive spectrum (Figure 6).

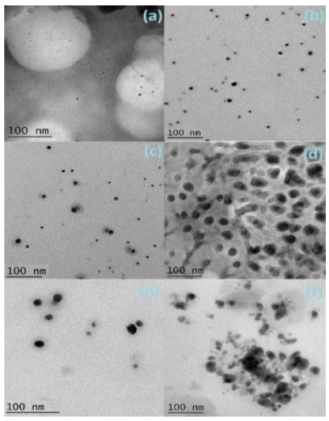


Figure 4. TEM micrographs of AgNPs.

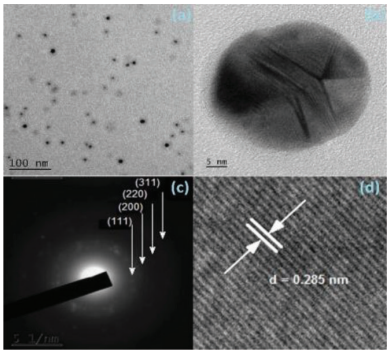


Figure 5. **(a)** Size distribution of AgNPs **(b)** HR-TEM micrographs of AgNPs **(c)** SAED pattern of AgNPs **(d)** Interplanar of AgNPs.

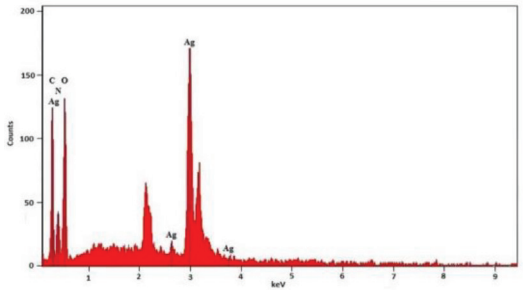


Figure 6. EDS spectra of AgNPs.

5.0 Conclusion

The accumulation of silk biomolecules over the surface of fabricated AgNPs, which were created under a controlled UV radiation environment, makes them more biocompatible. The formed nanoparticles are stable and uniformly dispersed. In the current article, we used UV-visible, TEM, and EDAX spectra to investigate the characteristic properties of nanoparticles that depend on their size, shape and morphology. Increased exposure duration can adjust the form and size of the nanoparticles, as seen by the absorption spectra, which show size variation as a function of irradiation time. The silver nanoparticles size, shape, diffraction pattern, and interplanar spacing are all fully revealed by the micrographs. The created nanoparticles are excellent for use in the manufacture of electronic devices and in biomedical filed.

6.0 References

1. Darroudi M, Ahmad MB, Zak AK, Zamiri R, Hakimi M. Fabrication and characterization of gelatin stabilized silver nanoparticles under UV-light. Int J Mol Sci. 2011; 12(9):6346-56. https://doi.org/10.3390/ijms12096346
2. Vaia RA, Maguire JF. Polymer nanocomposites with prescribed morphology: Going beyond nanoparticle-filled polymers. Chem Mater. 2007; 19(11):2736-51. https://doi.org/10.1021/cm062693+
3. Bang JH, Suslick KS. Applications of ultrasound to the synthesis of nanostructured materials. Adv Mater. 2009; 22(10):1039-59. https://doi.org/10.1002/adma.200904093
4. Liu G, Yang HG, Wang X, Cheng L, Pan J, Lu GQ, Cheng H. Visible light responsive nitrogen doped anatase TiO2 sheets with dominant {001} facets derived from TiN. J Am Chem Soc. 2009; 131(36):12868-9. https://doi.org/10.1021/ja903463q
5. McLaren A, Valdes-Solis T, Li G, Tsang SC. Shape and size effects of ZnO nanocrystals on photocatalytic activity. J Am Chem Soc. 2009; 131(35):12540-1. https://doi.org/10.1021/ja9052703

6. Aziz N, Faraz M, Pandey R, Shakir M, Fatma T, Varma A, Barman I, Prasad R. Facile algae-derived route to biogenic silver nanoparticles: Synthesis, antibacterial, and photocatalytic properties. Langmuir. 2015; 31(42):11605-12. https://doi.org/10.1021/acs.langmuir.5b03081
7. Aihara N, Torigoe K, Esumi K. Preparation and characterization of gold and silver nanoparticles in layered laponite suspensions Langmuir. 1998; 14(17):4945–9. https://doi.org/10.1021/la980370p
8. Temgire MK, Joshi SS. Optical and structural studies of silver nanoparticles. Radiat Phys Chem. 2004; 71(5):1039-44. https://doi.org/10.1016/j.radphyschem.2003.10.016
9. Murphy CJ, Sau TK, Gole AM, Orendorff CJ, Gao J, Gou L, Hunyadi SE, Li T. Anisotropic metal nanoparticles: Synthesis, assembly, and optical applications. J Phys Chem B. 2005; 109(29):13857-70. https://doi.org/10.1021/jp0516846
10. Hornebecq V, Antonietti M, Cardinal T, Treguer-Delapierre M. Stable silver nanoparticles immobilized in mesoporous silica. Chem Mater. 2003; 15(10):1993-9. https://doi.org/10.1021/cm021353v
11. Sun Y, Xia Y. Shape-controlled synthesis of gold and silver nanoparticles. Science. 2002; 298(5601):2176–9. https://doi.org/10.1126/science.1077229
12. Kora AJ, Manjusha R, Arunachalam J. Superior bactericidal activity of SDS capped silver nanoparticles: Synthesis and characterization. Mater Sci Eng C. 2009; 29(7):2104-9. https://doi.org/10.1016/j.msec.2009.04.010
13. Khanna PK, Singh N, Charan S, Viswanath AK. Synthesis of Ag/polyaniline nanocomposite via an in situ photo-redox mechanism. Mater Chem Phys. 2005;92(1):214-9. https://doi.org/10.1016/j.matchemphys.2005.01.011
14. Son WK, Youk JH, Park WH. Antimicrobial cellulose acetate nanofibers containing silver nanoparticles. Carbohydr Polym. 2006; 65(4):430-4. https://doi.org/10.1016/j.carbpol.2006.01.037
15. Guang-nian X, Xue-liang Q, Xiao-lin Q, Jian-guo C. Preparation and characterization of stable monodisperse silver nanoparticles via photoreduction. Colloids Surf A: Physicochem Eng Asp. 2008; 320(1-3):222-6. https://doi.org/10.1016/j.colsurfa.2008.01.056
16. Agnihotri S, Mukherji S, Mukherji S. Size-controlled silver nanoparticles synthesized over the range 5-100 nm using the same protocol and their antibacterial efficacy. RSC Adv. 2014; 4(8):3974-83. https://doi.org/10.1039/C3RA44507K
17. Dibrov P, Dzioba J, Gosink KK, Hase CC. Chemiosmotic mechanism of antimicrobial activity of Ag^{+} in ***vibrio cholerae.*** Antimicrob Agents Chemother. 2002; 46(8):2668-70. https://doi.org/10.1128/aac.46.8.2668-2670.2002
18. Shahverdi AR, Fakhimi A, Shahverdi HR, Minaian SS. Synthesis and effect of silver nanoparticles on the antibacterial activity of different antibiotics against *Staphylococcus aureus* and *Escherichia coli*. Nanomedicine. 2007; 3(2):168-171. https://doi.org/10.1016/j.nano.2007.02.001
19. Patil S, George T, Mahadik K. Green synthesized nanosilver loaded silk fibroin gel for enhanced wound healing. J Drug Deliv Sci Tech. 2015; 30:30-6. https://doi.org/10.1016/j.jddst.2015.09.001
20. Shivananda CS. Silk fibroin-based green colloidal silver nanoparticle synthesis and their antibacterial and anticancer properties. Inorg Chem Communi. 2023; 158(2):111611. https://doi.org/10.1016/j.inoche.2023.111611
21. Sarker SD, Nahar L, Kumarasamy Y. Microtitre plate-based antibacterial assay incorporating resazurin as an indicator of cell growth, and its application in the *in vitro* antibacterial screening of phytochemicals. Methods 2007; 42(4):321-4. https://doi.org/10.1016/j.ymeth.2007.01.006
22. Marignier JL, Belloni J, Delcourt MO, Chevalier JP. Microaggregates of non-noble metals and bimetallic alloys prepared by radiation-induced reduction. Nature. 1985; 317:344-5. https://doi.org/10.1038/317344a0
23. Darroudi M, Ahmad MB, Abdullah AH, Ibrahim NA, Shameli K. Effect of accelerator in green synthesis of silver nanoparticles. Int J Mol Sci. 2010; 11:3898-905. https://doi.org/10.3390/ijms11103898
24. Dong Q, Su H, Zhang D. *In situ* depositing silver nanoclusters on silk fibroin fibers supports by a novel biotemplate redox technique at room temperature. J Phys Chem B. 2005; 109(37):17429-34. https://doi.org/10.1021/jp052826z
25. Zhou Y, Chen W, Itoh H, Naka K, Ni Q, Yamane H, Chujo Y. Preparation of a novel core–shell nanostructured gold colloid–silk fibroin bioconjugate by the protein *in situ* redox technique at room temperature. Chem Commun. 2001; 23:2518-9. https://doi.org/10.1039/B108013J
26. Baia L, Baia M, Kiefer W, Popp J, Simon S. Structural and morphological properties of silver nanoparticles–phosphate glass composites. Chem Phy. 2006; 327(1):63-9. https://doi.org/10.1016/j.chemphys.2006.03.036
27. Esumi K, Hosoya T, Suzuki A, Torigoe K. Formation of gold and silver nanoparticles in aqueous solution of sugar-persubstituted poly(amidoamine) dendrimers. J Colloid Inter Sci. 2000; 226(2):346–52. https://doi.org/10.1006/jcis.2000.6849
28. Kweon HY, Um IC, Park YH. Structural and thermal characteristics of *Antheraea pernyi* silk fibroin or chitosan blend film. Polymer. 2001; 42(15):6651-6. https://doi.org/10.1016/S0032-3861(01)00104-5
29. Shivananda C S, Asha S, Madhukumar R, Satish S, Narayana B, Byrappa K, Wang Y, Sangappa Y. Biosynthesis of colloidal silver nanoparticles: Their characterization and antibacterial activity. Biomed Phy Eng Exp. 2016: 2(3):035004. https://doi.org/10.1088/2057-1976/2/3/035004